WIND TUNNEL TESTS OF THE UAG 92 170/SF SLOTTED FLAPPED WING SECTION

D. G. Marsden, Alberta, Canada

Presented at the XXIII OSTIV Congress, Borlänge, Sweden (1993)

Introduction

The UAG92 170/SF wing section was designed for the Minisigma variable geometry sailplane project. The 17% thickness was chosen for structural reasons because the variable geometry sailplane will have a high aspect ratio. A 25% chord slotted flap compared to the 35% chord flap used on Sigma makes the mechanical flap extension systems easier to build. A special feature of this wing section is the 15% chord aileron incorporated into the flap. This can be used as a combination camber flap and aileron. Wind tunnel tests were carried out to determine the basic airfoil characteristics, as well as optimum flap and aileron positions and angles. Aileron and flap hinge moments and derivatives showing aileron effectiveness with the flap retracted and flap extended were also measured.

Model

The one meter chord model was constructed using 0.8 mm thick aluminum alloy skins glued to a wood frame. This technique allows very accurate and wave free surfaces that are easily finished by painting and sanding smooth. Pressure taps were installed at mid span connecting directly to a scanivalve and pressure transducer. Measured surface static pressure coefficients were integrated to determine forces and moments on the model. The model was mounted vertically spanning the short dimension of the test section.

Figure 1 shows the shape of this wing section and the flap-aileron geometry, flap in and flap extended. Airfoil coordinates are given in Table I.

TABLE 1.

UAG92 170/SF

X	Yupper	Ylower
0.00000	0.00000	0.00000
0.00293	0.01007	-0.00711
0.01169	0.02189	-0.01272
0.02617	0.03464	-0.01855
0.04621	0.04763	-0.02360
0.07157	0.06078	-0.02807
0.10195	0.07360	-0.03212
0.13700	0.08552	-0.03584
0.17631	0.09620	-0.03870
0.21941	0.10530	-0.04112
0.26579	0.11254	-0.04344
0.31493	0.11783	-0.04523
0.36623	0.12104	-0.04662
0.41911	0.12198	-0.04783
0.47293	0.12056	-0.04869
0.52707	0.11665	0.04901
0.58089	0.11010	-0.04877
0.63376	0.10065	-0.04799
0.68507	0.08831	-0.04628
0.73420	0.07329	-0.04255
0.78059	0.05516	-0.03653
0.82369	0.03655	-0.03000
0.86300	0.02275	-0.02327
0.89805	0.01754	-0.01426
0.92843	0.01250	-0.00795
0.95379	0.00855	-0.00393
0.97383	0.00543	-0.00156
0.98831	0.00293	-0.00041
0.99707	0.00104	0.00001
1.00000	0.00000	0.00000

Wind Tunnel and Instrumentation

The 1.22 by 2.44 meter rectangular test section can provide Reynolds number up to $2.1*10^6$ for the 1 meter chord model. Turbulence intensity is generally about 0.1%, but rises sharply at the highest tunnel speed. In view of this, the maximum Reynolds number tested was kept to 1.8 million. For comparison[1], the free stream turbulence level of some other airfoil tunnels are: NASA Langley Low Turbulence Pressure Tunnel, 0.1%, Delft University, 0.06%, and the Stuttgart University tunnel, 0.02%.

A data acquisition system operated by a small computer was used to take measurements and reduce the data. Pressure distributions were measured using a scanivalve together with a sensitive differential pressure transducer. Wind tunnel speed was measured using a pitot tube located just ahead of the test section, calibrated against a pitot tube located at the model position in an empty test section. Drag was measured using a pitot

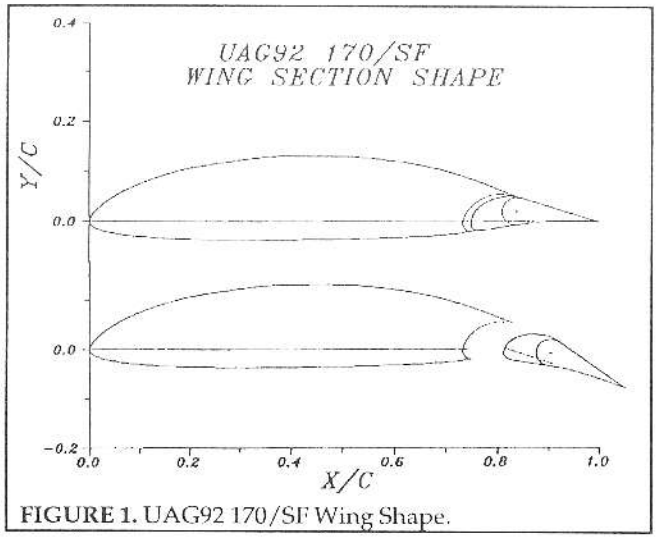

FIGURE 1. UAG92 170/SF Wing Shape.

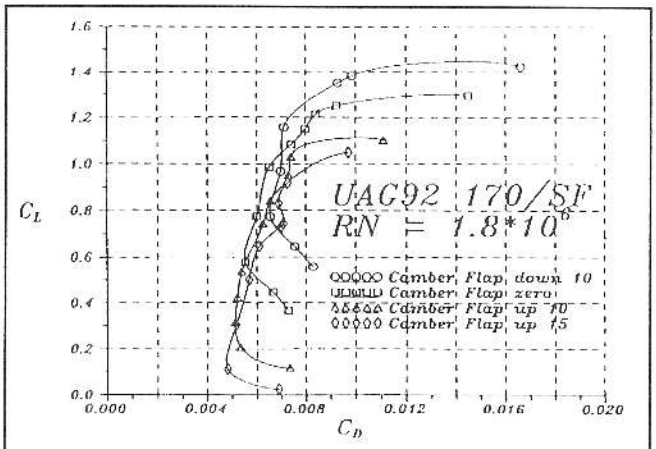

FIGURE 2a. Lift-Drag at Reynolds Number $1.8*10^6$

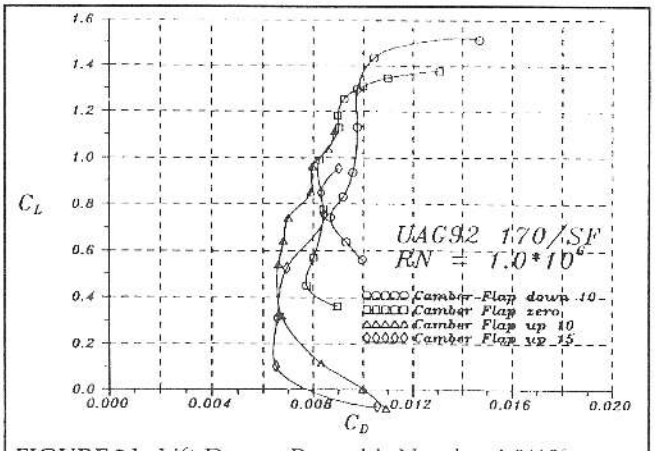

FIGURE 2 b. Lift-Drag at Reynolds Number $1.0*10^6$.

tube traversed through the wake at a position 0.5 meters behind the model trailing edge. The Micro Switch series 160PC transducers which were used are very stable and very linear.

Repeatability is very good, even at the very low dynamic pressures required for a Reynolds number of $0.5*10^6$.

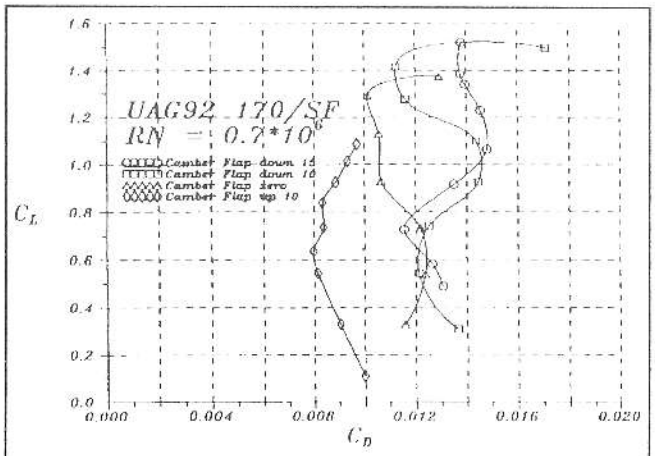

FIGURE 2 c. Lift-Drag at Reynolds Number $0.7*10^6$.

A standard laboratory pitot-static tube with a diameter of 4 mm is used for the wake traverse. This is mounted on a long sting so that the traverse mechanism is clear of the wake. Wake thickness at the measuring station is typically about 80 mm. Figure 3 shows a schematic of the pressure measurement system.

The Betz equation for wake drag is given by:[2]

$$C_D = \int \frac{g_\infty - g_2}{q_\infty} d\left(\frac{y}{l}\right) + \int \left(\sqrt{\frac{g_\infty - p_2}{q_\infty}} - \sqrt{\frac{g_2 - p_2}{q_\infty}}\right)\left(\sqrt{\frac{g_\infty - p_2}{q_\infty}} + \sqrt{\frac{g_2 - p_2}{q_\infty}} - 2\right) d\left(\frac{y}{l}\right)$$

where

q_∞ = free stream dynamic pressure averaged over the traverse time

$g_\infty - g_2$ = total head pressure outside the wake - wake total pressure

$g_\infty - P_2$ = total head pressure outside the wake - wake static pressure

$g_2 - P_2$ = wake total pressure - wake static pressure

Total head pressure outside the wake is taken to be the average of values of g_2 measured just at the top and bottom edges of the wake during a traverse.

The model chord to height ratio is c/h = 0.4. Conventional linear corrections[3] for blockage and flow curvature have been programmed into the data reduction procedure.

Results and Discussion

Drag Measurements - Flap retracted

Lift - drag results are shown in figures 2(a),(b),(c), for Reynolds numbers $1.8*10^6$, $1.0*10^6$, and $0.7*10^6$ respectively, for a range of settings of the camber flap. The flap up 10 degrees appears to be the best setting over most of the speed range. Figure 3 shows an envelope of drag curves for three Reynolds numbers, derived from Figure 2.

Flight Polars

While it is convenient to measure drag characteristics at a constant Reynolds number in the wind tunnel, for an

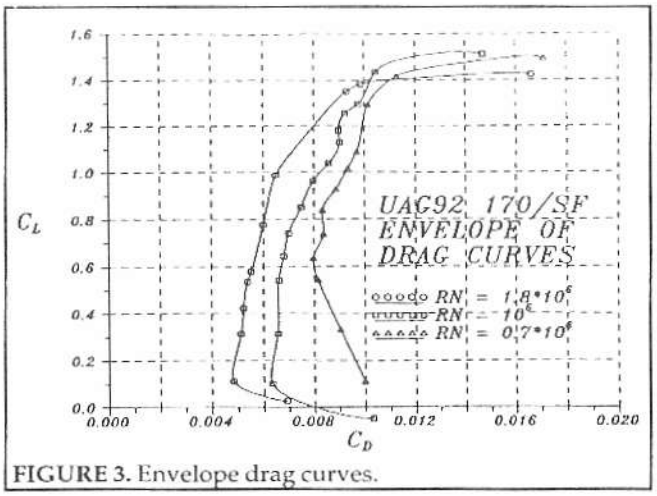

FIGURE 3. Envelope drag curves.

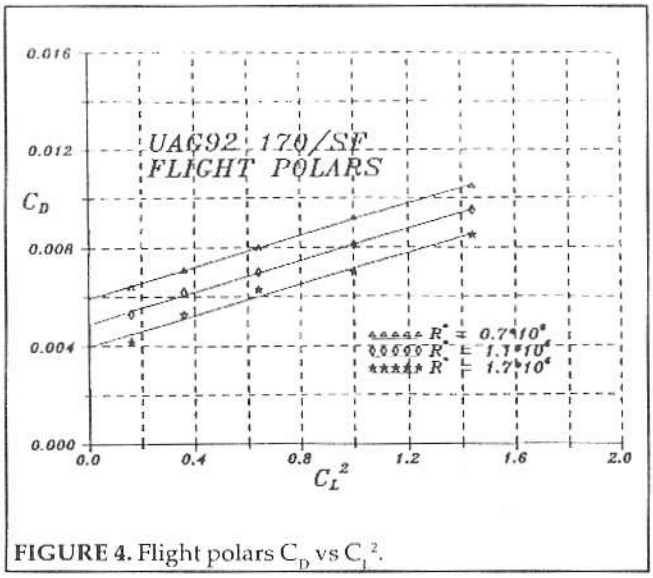

FIGURE 4. Flight polars C_D vs C_L^2.

aircraft in flight both lift coefficient and Reynolds number will depend on flight speed. Representation of the drag results in terms of flight polars will give a better appreciation of the airfoil characteristics as they will be seen in a practical application. Reynolds number will also depend on wing chord and wing loading. If we introduce a characteristic Reynolds number, R* = Reynolds number when the lift coefficient is 1.0,

$$R^* = \frac{c}{\mu}(2\rho W/S)$$

and

$$R = \frac{R^*}{\sqrt{C_L}}$$

where,

c = wing chord
W/S = wing loading
μ = viscosity of air
ρ = air density

It can be shown[4] that R* for typical competition sailplanes lies in the range from $1.7*10^6$ to $0.7*10^6$ representing root chord with maximum water ballast, and tip chord with no water ballast respectively. A good average value based on mean chord and no water ballast is $R^* = 1.1*10^6$.

Flight polars for the UAG92 170/SF airfoil, obtained by interpolation of the data in Figure 3, are plotted as C_D against C_L^2 in Figure 4. The data form good straight lines, which allow an analytical expression for wing section drag that will be useful in analysis of sailplane performance.

Drag can be represented as:

$$C_D = 0.005 / \sqrt{R^*} + 0.0033\, C_L^2$$

Using a value of R* based on mean wing chord makes the implicit assumption that drag characteristics are linear with Reynolds number. The envelope curves in Figure 4 confirms that this is a reasonable assumption in the Reynolds number range from 0.7 to 1.8 million. Use of R* based on mean chord should be a good approximation in calculating sailplane performance.

Drag Measurements - Flap Extended

Drag results with the flap extended at a deflection of 20 degrees with the aileron zero and up 10 degrees are shown in Figure 5. Lift and drag coefficients are based on flap retracted chord. The aileron in this case is also the camber flap. When the flap is retracted the aileron - camber flap operates in the same manner as it would on a wing section with no slotted flap. While the increase in lift appears moderate compared to flap retracted, the stall characteristics of the slotted flap airfoil allows the sailplane to be flown at a lift coefficient of 1.8 without any danger of stalling or loss of aileron control. Stall occurs as a separation on the trailing edge of the main wing section, with the flap continuing to have attached flow maintaining aileron control power.

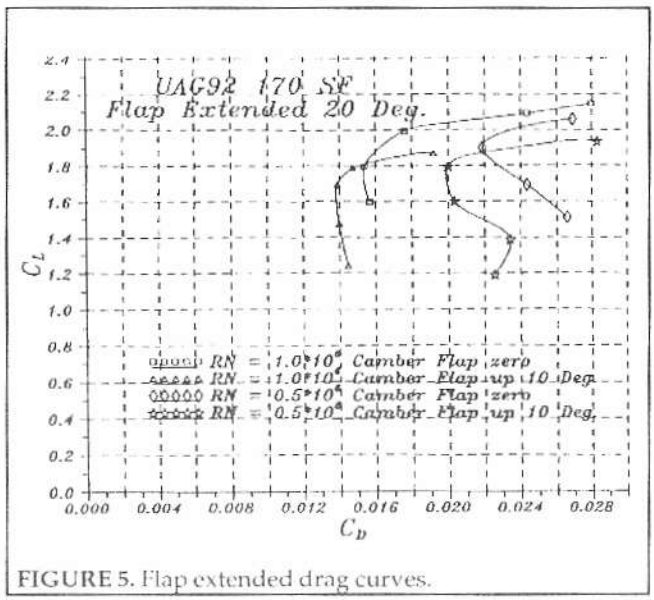

FIGURE 5. Flap extended drag curves.

Lift

Flap retracted lift curves are shown in Figure 6, for Reynolds number $1.0*10^6$. These curves show the very mild stall characteristic of this airfoil resulting from the trailing edge type stall.

The flap extended lift curves are shown in Figure 7 for two Reynolds numbers. There is a small reduction of lift at the lower Reynolds number of $0.5*10^6$, but otherwise the curves are similar. The mild stall characteristics are again evident. The drag results suggest optimum operation at a lift coefficient of 1.8 which is well below the maximum lift, even with the aileron/camber flap in the 10 degree up position.

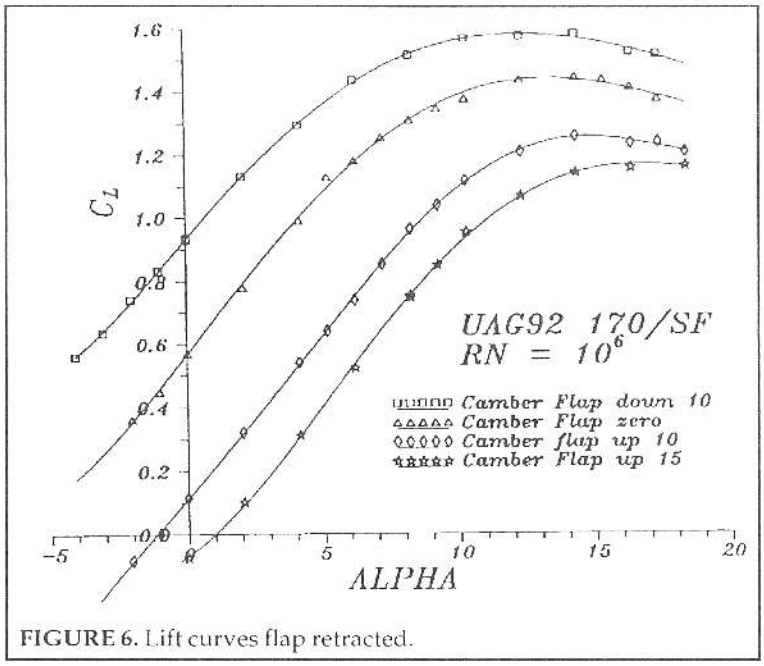

FIGURE 6. Lift curves flap retracted.

Moment Coefficients

Pitching moment about the quarter chord is shown in Figures 8 and 9 for a range of flap deflections. They do not change appreciably with Reynolds number.

Aileron Effectiveness

A cross plot of lift coefficient against aileron angle shows values of $dC_L / d\delta_a = 0.0375$ per degree for the flap retracted, and $dC_L / d\delta_a = 0.043$ per degree with the flap extended. Aileron control effectiveness is somewhat better with the flap extended. Aileron effectiveness with the flap extended is a major advantage of the slotted flap wing section for use on variable geometry sailplanes.

Pressure distributions

Measured pressure distributions provide additional information that is not obtained when lift forces are measured directly. For example, comparison of pressure distributions measured at Reynolds number $1.8*10^6$ and $0.7*10^6$ for the same angle of attack in Figure 10 shows laminar bubble separations on both the top and bottom at the lower Reynolds number. The series of pressure distributions shown in Figure 11 for RN = $0.7*10^6$ show the upper surface laminar separation bubble gradually disappearing while the lower surface bubble remains. This situation appears to be an ideal application for some kind of boundary layer trip to reduce the effect of the laminar bubbles. Zig-zag tape boundary layer trips were used to try to eliminate the laminar bubbles, and this did decrease drag in some cases at the lower Reynolds numbers, but for most cases the boundary layer trips resulted in increased drag.

Pressure distributions with the camber flap up 15 degrees showed attached flow to the trailing edge as would also be indicated by the low values of profile drag coefficient. Camber flap up tends to eliminate the laminar separation on the lower surface, making a boundary layer trip unnecessary.

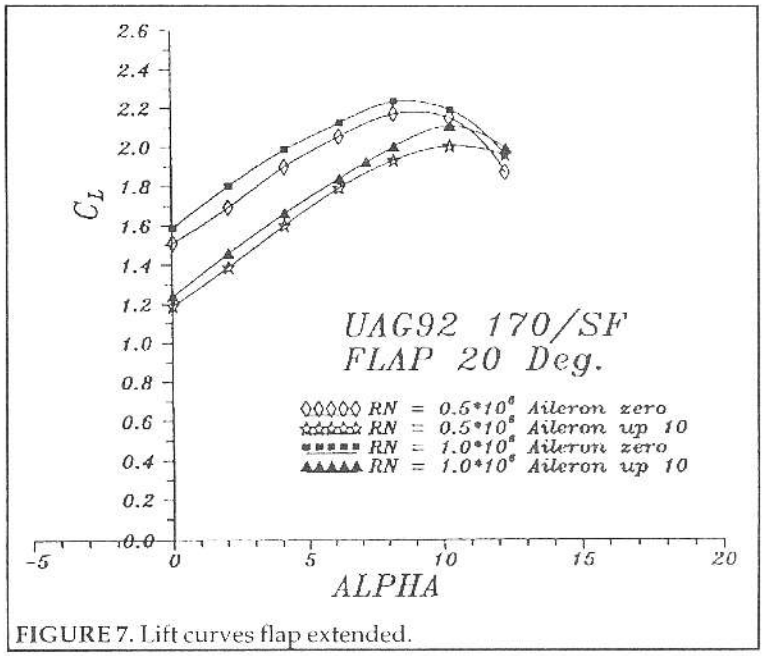

FIGURE 7. Lift curves flap extended.

Pressure distributions with the flap extended at 20 degrees with the camber flap at zero, showed that there is almost no change in pressure distribution on the flap until some separation takes place on the main section at the highest angle shown. In this example the maximum lift coefficient is 2.2 at 8 degrees angle of attack, and decreasing at higher angles, as shown in Figure 7. The optimum operational range would be at 2 to 4 degrees angle of attack since the drag increases sharply for angles greater then 4 degrees.

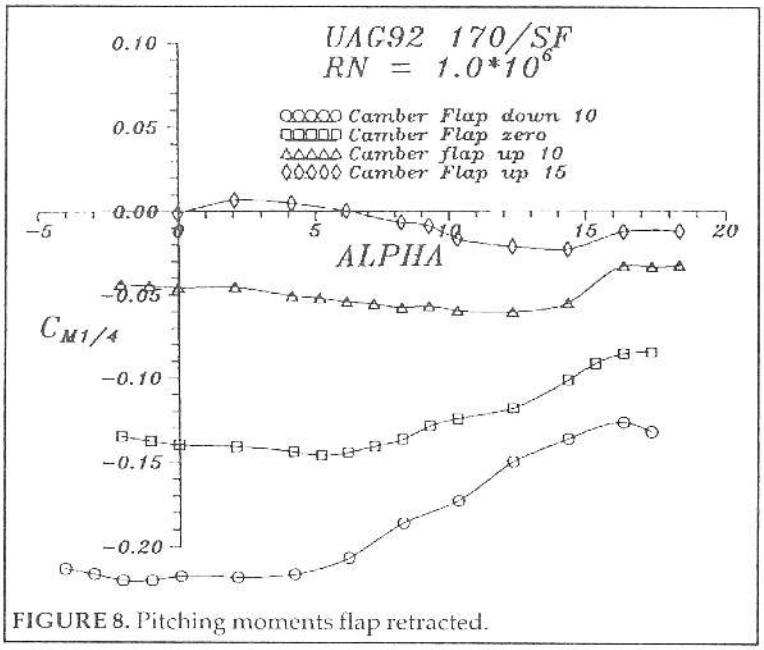

FIGURE 8. Pitching moments flap retracted.

some roughness at the flap joints not present in the original FX model.

Figure 13 shows a comparison of Flap extended results measured in the U of A wind tunnel with the original FX 67 VC 170/36 results measured in the Stuttgart wind tunnel[5]. The flap extended results from Reference 5 have been translated to reflect lift and drag coefficients (and Reynolds number) based on flap retracted chord. Flap extended results for the slotted flapped version of the FX 67 VC 170 airfoil, measured in the U of A wind tunnel are also shown for comparison. Clearly, the unslotted flap has the best performance as shown on this graph. However, flight test experience with the Sigma experimental sailplane showed that the improved aileron control possible with the slotted flap was more important than the difference in profile drag which is small relative to overall aircraft drag. Flap extended

Comparisons

Performance of the UAG92 170/SF slotted flapped wing section are compared to published results[5] for the FX 67 VC 170/36 and with results for the slotted flapped version of this wing section which were measured in the U of A wind tunnel. Figure 12 shows a comparison of the results for the FX 76 VC 170/36 wing section measure in the U of A wind tunnel with the original Stuttgart measurements. The results are in reasonable agreement. The differences are probably due to differences in the model. The model used in this case was the slotted flap version of FX67 VC 170 used on Sigma with the flap retracted, which has

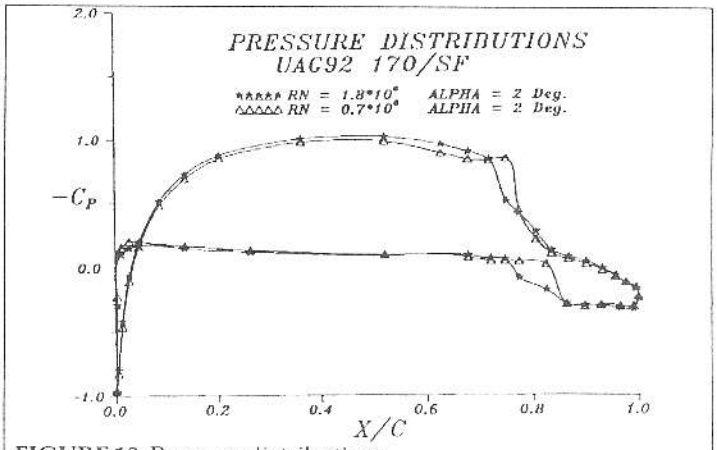

FIGURE 10. Pressure distributions.

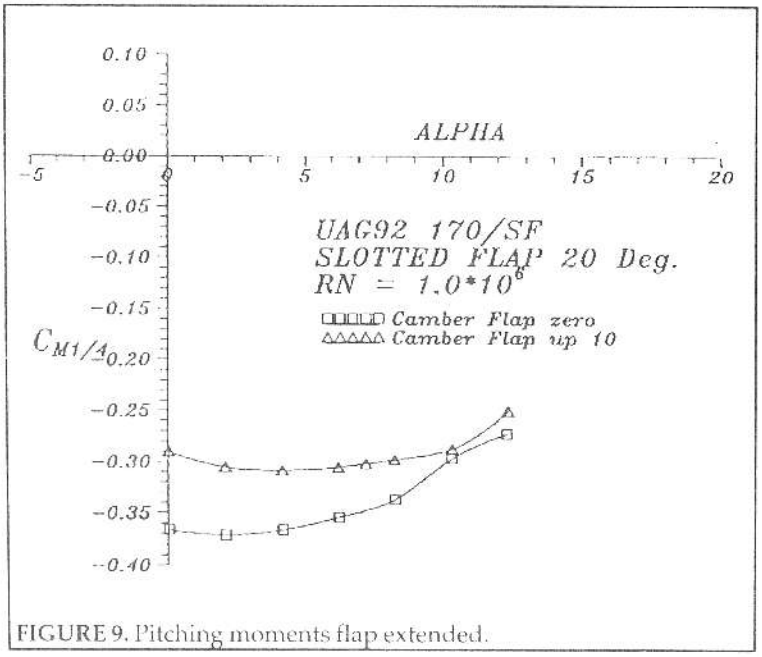

FIGURE 9. Pitching moments flap extended.

results for the UAG92 wing section lie between the slotted and unslotted Wortman airfoil results, and should produce performance similar to the slotted FX wing section results in a practical application.

Conclusion

Wind tunnel tests have been carried out to determine the characteristics of the UAG92 170/SF slotted flap wing section for use on variable geometry sailplanes. This wing section depends on a camber flap to obtain a wide range of operational lift coefficient, and would be mostly operated with the camber flap deflected up.

Flap extended lift - drag characteristics of this wing section are comparable to slotted flapped version of the FX 67 VC 170/36 wing section used on the Sigma variable geometry sailplane. Drag coefficient for this wing section lies between that

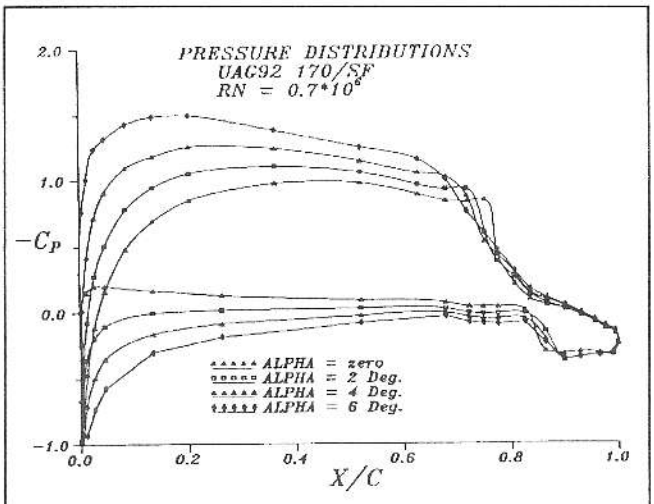

FIGURE 11. Pressure distributions.

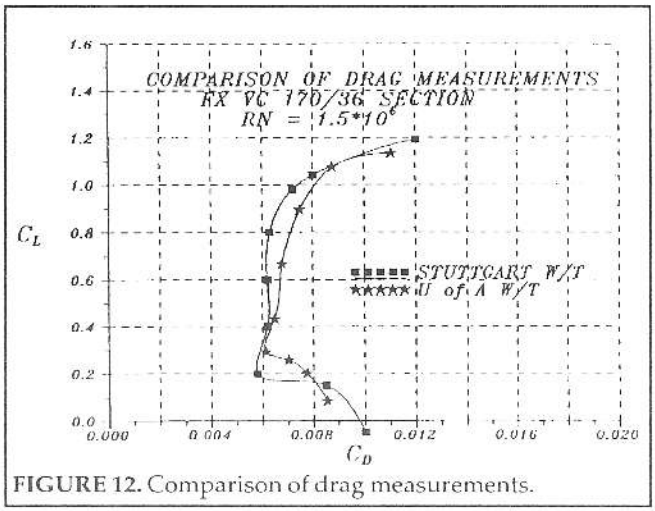

FIGURE 12. Comparison of drag measurements.

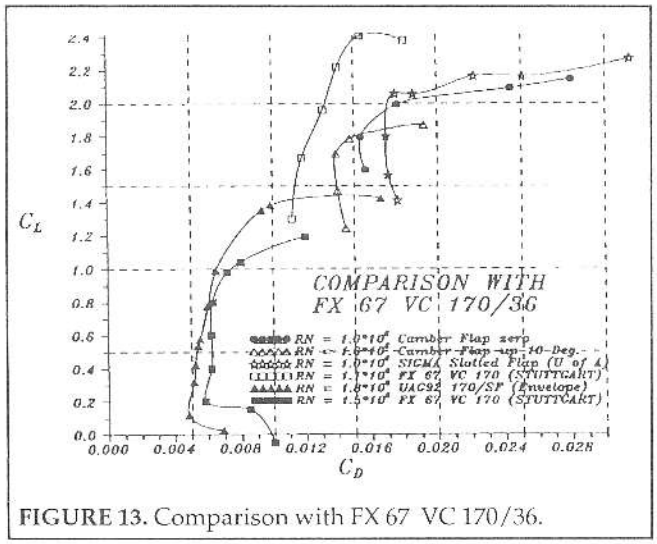

FIGURE 13. Comparison with FX 67 VC 170/36.

of the unslotted and slotted flap versions of the FX 67 VC 170 wing section.

These wind tunnel tests show that the UAG92 170/SF wing section would be a good choice for a variable geometry sailplane using a slotted flapped wing section.

References

1. J.L. Van Ingen and L.M.M. Boermans "Aerodynamics at Low Reynolds Numbers: A Review of Theoretical and Experimental Research at Delft University of Technology," International Conference on Aerodynamics at Low Reynolds Number, Vol. 1, Royal Aeronautical Society, London, October, 1986.
2. H. Schlichting, *Boundary Layer Theory*, Pergamon Press Ltd., Chapter 24, Pages 507 to 511, 1955.
3. Alan Pope and John J. Harper, *Low-Speed Wind Tunnel Testing*, John Wiley and Sons, 1966.
4. D. J. Marsden "Wind Tunnel Tests of an Ultralight Sailplane Wing Section," *Technical Soaring*, Vol. 14, No. 1, 1990.
5. D. Althaus, *Stuttgarter Profilkatalog 1*, 1972